Foundation, Polymers Program, which provided computer time at the supercomputer centers at the University of Minnesota and at the University of Illinois.

(2) de Gennes, P.-G. *Scaling Concepts in Polymer Physics*; Cornell University: Ithaca, NY, 1979.
(3) Flory, P. J. *J. Chem. Phys.* **1949**, *17*, 303.
(4) Daoud, M.; Cotton, J. P.; Farnoux, B.; Jannink, G.; Sarma, G.; Benoit, H.; Duzlessix, R.; Picot, C.; de Gennes, P.-G. *Macromolecules* **1975**, *8*, 804.
(5) Curro, J. G. *J. Chem. Phys.* **1974**, *61*, 1203. Khalatur, P. G.; Papulov, Yu. G.; Pavlov, A. S. *Mol. Phys.* **1986**, *58*, 887.
(6) Curro, J. G. *Macromolecules* **1979**, *12*, 463.
(7) Ullman, R. *Macromolecules* **1986**, *19*, 1748. Our notation differs from this reference in that brackets denote long-time averages for a single chain.
(8) For historical and general presentations of the theory, see: Flory, P. J. *Theory of Polymer Chemistry*; Cornell University: Ithaca, NY, 1953. Treloar, L. R. G. *The Physics of Rubber Elasticity*, 3rd ed.; Clarendon: Oxford, 1975. Recent reviews are given by: Eichinger, B. E. *Annu. Rev. Phys. Chem.* **1983**, *34*, 359. Ullman, R. *J. Polym. Sci., Polym. Symp.* **1985**, *72*, 39.
(9) Flory, P. J. *Proc. R. Soc. London, A* **1976**, *351*, 351.
(10) Ronca, G.; Allegra, G. *J. Chem. Phys.* **1975**, *63*, 4990.
(11) Flory, P. J.; Erman, B. *Macromolecules* **1982**, *15*, 800.
(12) Mark, J. E.; Curro, J. G. *J. Chem. Phys.* **1983**, *79*, 5705.
(13) Gao, J.; Weiner, J. H. *Macromolecules*, preceding paper in this issue.
(14) James, H. M.; Guth, E. *J. Polym. Sci.* **1949**, *4*, 153.
(15) In an earlier paper (Gao, J.; Weiner, J. H. *J. Chem. Phys.* **1984**, *81*, 6176) it was stated (ref 3) that a term of the form $F_E(v,T)$ could make an anisotropic contribution to the stress tensor when the stretch ratios are unequal. This is only correct for the form of the stress tensor referred to the original area. For the usual stress tensor, referred to the present area, the contribution is hydrostatic.
(16) Boggs, F. W. *J. Chem. Phys.* **1952**, *20*, 632.
(17) Eichinger, B. E. *Macromolecules* **1981**, *14*, 1071.
(18) DiMarzio, E. A. *J. Chem. Phys.* **1962**, *36*, 1563.
(19) Jackson, J. L.; Shen, M. C.; McQuarrie, D. A. *J. Chem. Phys.* **1966**, *44*, 2388.
(20) Gaylord, R. J. *Polym. Eng. Sci.* **1979**, *19*, 263.
(21) See, for example: Weiner, J. H. *Statistical Mechanics of Elasticity*; Wiley: New York, 1983; pp 234–237.
(22) Gao, J.; Weiner, J. H. *Macromolecules* **1987**, *20*, 142.
(23) Treloar, L. R. G. *The Physics of Rubber Elasticity*, 3rd ed.; Clarendon: Oxford, 1975; pp 113–116.
(24) Chandler, D.; Weeks, J. D.; Andersen, H. C. *Science (Washington, D.C.)* **1983**, *220*, 787.
(25) Flory, P. J. *Statistical Mechanics of Chain Molecules*; Interscience: New York, 1969; p 315.
(26) Weiner, J. H.; Berman, D. H. *J. Chem. Phys.* **1985**, *82*, 548.
(27) Berman, D.; Weiner, J. H. *J. Chem. Phys.* **1985**, *83*, 1311.
(28) Lecture notes by A. Rahman, Aug 2, 1985, unpublished results. Sullivan et al. (Sullivan, F.; Mountain, R. D.; O'Connell, J. *J. Comp. Phy.* **1985**, *61*, 138) provided useful guides to vectorizable algorithms for molecular dynamics calculations.

Ultimate Elastic Modulus and Melting Behavior of Poly(oxymethylene)

J. Runt,* R. F. Wagner, and M. Zimmer

Polymer Science Program, Department of Materials Science and Engineering, The Pennsylvania State University, University Park, Pennsylvania 16802.
Received February 9, 1987

ABSTRACT: The ultimate crystalline modulus of poly(oxymethylene) was estimated by using the Raman longitudinal acoustic mode and small-angle X-ray scattering. In this paper we emphasize the sensitivity of the calculated modulus to the values chosen for the thickness of the crystalline regions. Assuming that the uniform elastic rod model provides an adequate description of the LAM, we found E_c = 146 GPa, in excellent agreement with the results of neutron-scattering experiments. We have also explored the melting behavior of the solution-crystallized materials used in this study. The estimated value of the fold surface free energy ($\doteq$88 ergs/cm^2) indicates a work of chain folding near 4 kcal/mol folds, a value in line with that found for other polyethers.

Introduction

Some 40 years ago, Mizushima and Shimanouchi[1] observed a band in the low-frequency Raman spectra of crystalline *n*-alkanes whose peak position varied inversely with the paraffin chain length. This band was assigned to a longitudinal accordion-like motion of the *n*-alkane chains and has been termed the longitudinal acoustic mode (LAM). Using an analogy with the case of a simple elastic rod, they found that the LAM peak frequency (ν) was related to the paraffin chain length (l) by

$$\nu = \frac{m}{2cl}\left(\frac{E}{\rho}\right)^{1/2} \quad (1)$$

where m is the mode order, c is the speed of light, and E and ρ the elastic modulus and density of the elastic rod.

Since this initial work, LAM's have been observed for a number of semicrystalline polymers.[2] In crystalline polymers, the accordion-like vibration is usually envisioned as being decoupled at the "interface" between the crystal core and fold surface and, as a consequence, l in eq 1 is taken as the crystalline thickness and E and ρ should correspond to E_c and ρ_c, the modulus and density of the crystalline core.

Since ρ_c is generally known and if the simple elastic rod model provides an adequate description of polymeric LAMs, measurement of l and ν can yield E_c directly. For the semicrystalline polymers studied thus far, the values of E_c determined by the LAM–uniform elastic rod approach agree quite well with those determined from neutron-scattering measurements.[3,4] However, a rather large discrepancy often exists between these values and those determined from X-ray crystal strain measurements. It appears that the primary assumption employed in the X-ray analysis (i.e., that the stress applied to the specimen is distributed homogeneously) is not a good approximation. This is the implication from the work of Brew et al.,[5] who examined the apparent crystal modulus of polyoxymethylene (POM) by the X-ray technique. The apparent modulus was found to vary from 44 GPa at room temperature to 105 GPa at −165 °C. The authors regard this latter value as a lower limit for the true E_c if at −165 °C the amorphous modulus is significantly less than E_c.[5]

In studies where ultimate crystalline moduli have been derived from LAM experiment, melt-crystallized or annealed specimens have been frequently employed. The microstructure of these materials is generally quite complex and this complicates, for example, the assessment of

0024-9297/87/2220-2531$01.50/0

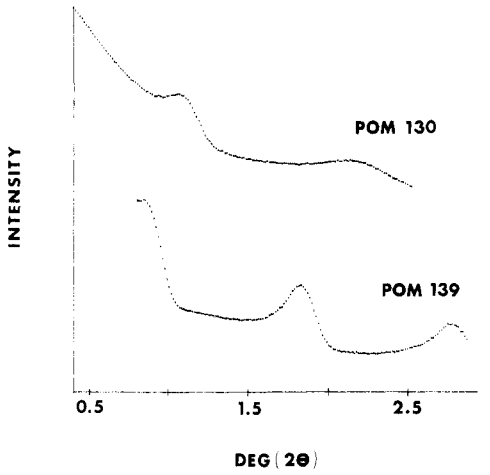

Figure 1. Small-angle X-ray scattering patterns of POM 130 and 139.

l from the small-angle X-ray scattering (SAXS) long period. Care must also be taken to apply the appropriate corrections to the SAXS and LAM data. In this paper we report the results of a LAM study on relatively well-defined poly(oxymethylene) single crystals. Particularly, we emphasize the sensitivity of the derived E_c to the values chosen for l and the special care required before LAM-derived ultimate moduli can be quoted with confidence. In addition, we also report an investigation of the melting behavior of the POM single crystals.

Experimental Section

Single crystals of poly(oxymethylene) (Delrin 500) were grown isothermally from a 0.05% solution of the polymer in *o*-dichlorobenzene at 130, 135, 139, and 142 °C by using a self-seeding technique.[6] After washing at the crystallization temperature (T_c) with fresh *o*-dichlorobenzene, the preparation was cooled to room temperature. A portion of each preparation was then transferred to xylene by washing and centrifugation, and oriented mats were formed under the force of gravity. The mats were washed with acetone and dried under vacuum (5×10^{-5} Torr) at room temperature for 2 days. Another portion of each preparation was transferred to acetone by the same procedure and the acetone allowed to evaporate, leaving a powder of the single crystals. These single-crystal powders were also dried under vacuum for 2 days.

The fold period (L) of the crystals from each preparation was obtained from small-angle X-ray scattering measurements by using a slit-collimated Kratky camera. The resulting X-ray patterns were corrected for background scattering and Lorentz corrected by using a $(2\theta)^2$ term.

The single-crystal powders were placed in glass capillaries and the low-frequency Raman spectra obtained with a Jobin-Yvon HG2S Raman Spectrometer. An argon ion laser was used as the light source and a resolution of 3 cm^{-1} was used for all samples. The experimental spectra were corrected for background scattering by subtracting a best-fit base line and the resulting intensities were then corrected for both temperature and frequency effects.[7,8]

The melting point (T_m) and heat of fusion (ΔH_f) for crystals grown at the different T_c's were determined with a Perkin-Elmer differential scanning calorimeter (DSC-2). To avoid difficulties associated with low thermal conductivity,[9] sample sizes of less than 0.1 mg were used for determination of T_m. Quantities of 0.3–0.5 mg were used for ΔH_f measurements. A heating rate of 20 deg/min was used unless otherwise noted. Melting points and heats of fusion were corrected with an indium standard.

Results and Discussion

A. SAXS and Thermal Analysis. The background- and Lorentz-corrected SAXS patterns of two of the single-crystal preparations are shown in Figure 1. Several orders of reflection are easily observed. In fact, examination of the scattering out to higher angles than shown in Figure 1 shows at least five orders of reflection for

Table I
Fold Period, Heat of Fusion, and Melting Point of Poly(oxymethylene) Single Crystals

T_c	L, Å	ΔH_f, cal/g	T_{M_1}, °C	T_{M_2}, °C
130	76	41	162.3	169.9
135	94	48	165.2	174.0
139	97	48	165.9	174.7
142	111	53	167.7	~173

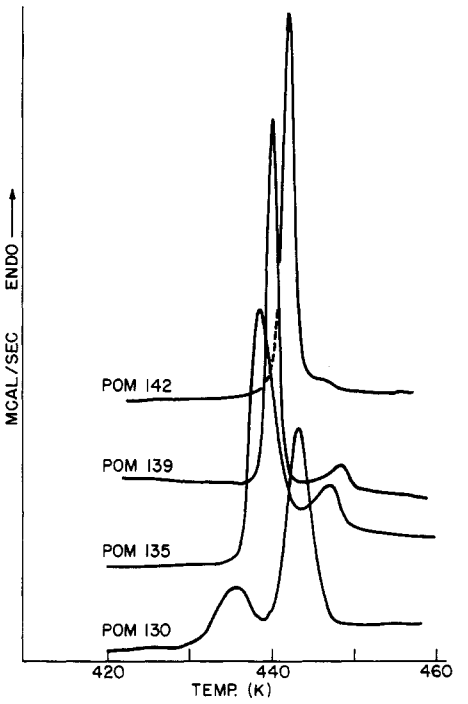

Figure 2. Melting behavior of all single-crystal samples. Heating rate = 20 deg/min.

crystals grown at 139 °C.[10] The fold periods of each sample (Table I) were obtained from the most intense and well-resolved peak in each pattern. This was usually the second-order reflection since the first order was often somewhat obscured by the unusually high scattering intensity at very low angles. For crystals grown under identical conditions as those employed in this study, Khoury and Barnes[6] found that the procedure of washing the crystals at T_c caused a mild and selective etching of the crystal lamellae. They observed the formation of randomly dispersed holes (approximately 0.03–0.16 μm in diameter) in the interior of the POM crystals which preferential orientation parallel to the outer edge of the crystals. SAXS of such crystals would be expected to show significant diffuse scattering from the holes and this is presumably the source of the unusually high intensity observed at low angles in Figure 1.

Representative DSC thermograms of crystals formed at the four T_c's are shown in Figure 2. Multiple melting endotherms are observed for all samples. This behavior is similar to that seen previously for POM crystals grown under somewhat different conditions than reported here.[11] The first melting peak for crystals formed at 139 and 142 °C is extremely sharp, exhibiting a width at half-peak height of only about 1.6 deg. The melting points of the lower (T_{m_1}) and upper temperature (T_{m_2}) endotherms generally increase with increasing T_c (Table I). In addition, the magnitude of the lower temperature endotherm increases relative to the upper melting peak as T_c increases. This is what would be expected if the multiple-melting behavior originated in a mechanism in which the "original" crystals (i.e., formed at T_c) melt, recrystallize, and then remelt; i.e., the originally thicker crystals would be less

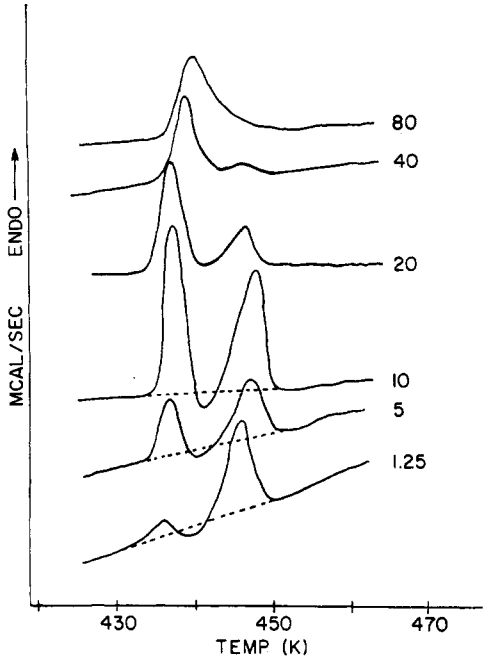

Figure 3. Heating rate dependence of melting behavior of POM 135.

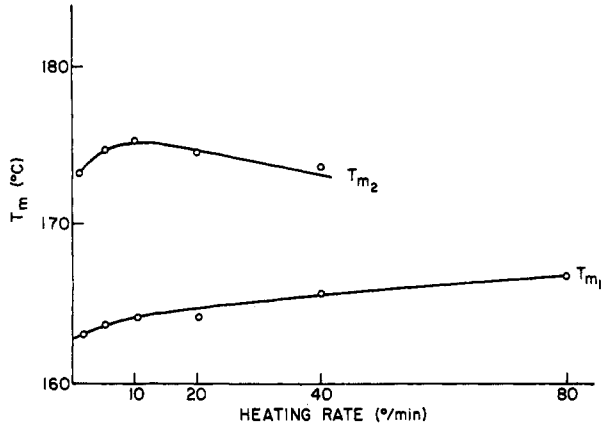

Figure 4. Plot of lower and upper melting temperatures of POM 135 as a function of heating rate.

inclined to thicken during heating in the DSC. To explore this possibility further, heating rate experiments were conducted on crystals grown at 135 °C (Figure 3). Clearly, the lower temperature endotherm increases in relative magnitude and position (Figure 4) as heating rate increases. Exothermic responses can be detected at heating rates from 1.25 to 10 deg/min. This behavior fits well with expectations from a model based on initial melting, recrystallization, and subsequent remelting.[12,13] The true melting point (i.e., the T_m of the original crystals) can, in principle, be obtained at rates high enough to completely suppress crystal thickening during heating. However, low polymer thermal conductivity and the possibility of superheating frequently make assessment of the true T_m at high heating rates unreliable.

The equilibrium melting point ($T_m°$) was estimated from a Hoffman–Weeks plot[14] of T_m vs. $1/l_c$ where l_c is the crystalline thickness, assuming that T_{m_1} at 20 deg/min is a resonable approximation for the true T_m. l_c was obtained from $L - l_a$, where L is the measured fold period and l_a is the total amorphous surface layer thickness. An analysis of the number of Bragg reflections in the SAXS patterns of the POM crystals used in this study suggests that l_a has a maximum of 18 Å for these crystals.[10] As a first approximation, l_a was assumed to be equal to 18 Å for all the

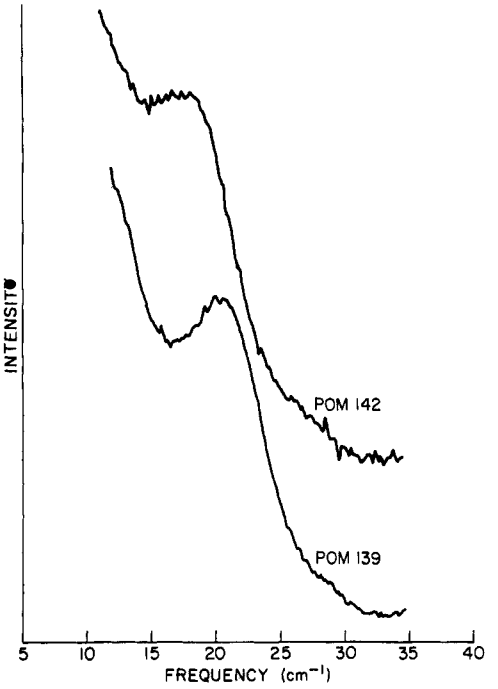

Figure 5. Experimental Raman spectra for POM 139 and 142.

single crystals used in this study. Regardless of whether $1/l_c$ or $1/L$ was used in the Hoffman–Weeks analysis, $T_m°$ was found to be 177–180 °C, in good agreement with the results from a number of investigations.[15] However, this value is some 20 deg lower than the extrapolated $T_m°$ obtained for melt-crystallized samples[16] and an experimentally observed T_m of extended-chain POM.[17] The reason for this discrepancy is unknown at this time.

The end or fold surface free energy (σ_e) can also be derived from the Hoffman–Weeks plot but the values obtained from such an analysis can depend strongly on the value chosen for $\Delta H_f°$ (the equilibrium heat of fusion) and the amorphous surface layer thickness. Estimates of $\Delta H_f°$ fall into two categories: approximately 59[18,19] and 77 cal/g.[20,21] As discussed below, we feel that a value of 59 cal/g is more reasonable. Using l_a = 18 Å, we find σ_e = 88 ergs/cm^2. This agrees well with a number of previous reports[15] but is about one-half of that derived recently from a reanalysis of previously published growth rate data.[22]

The work of chain folding can be estimated from σ_e by[23]

$$2ab\sigma_e = q \qquad (2)$$

where a and b are the width and thickness of a chain stem, respectively. Taking ab equal to 17.15 Å^2,[23] we obtain q = 4.3 kcal/mol folds, a value which is roughly in line with that calculated for other polyethers.[23]

The heats of fusion of crystals from each preparation are also shown in Table I. Degrees of crystallinity of 70–90% were calculated by using $\Delta H_f°$ = 59 cal/g while values ranging from 53 to 68% are obtained for $\Delta H_f°$ = 78 cal/g. The former values are more typical of single crystals and are much closer to the value reported for POM single crystals reported by Jaffe and Wunderlich.[11]

B. Longitudinal Acoustic Mode. Figure 5 shows the experimental low-frequency Raman spectra of two representative POM samples (grown at 139 and 142 °C). The peak observed in this region of the spectra decreases in frequency with increasing T_c (larger fold period) and was therefore assigned to the longitudinal acoustic mode. Table II lists the frequency- and temperature-corrected LAM peak frequencies for all samples after background subtraction. The corrections do not cause large changes in peak frequency for these relatively narrow bands, the

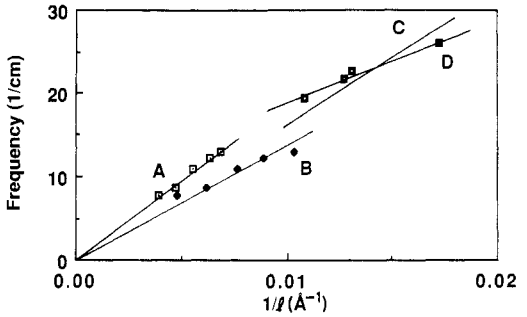

Figure 6. Plot of LAM peak frequency vs. $1/L$ or $1/l_c$: (A) data from ref 25; (B) replotted data from ref 25 assuming $l_c = L - 50$ Å; (C) regression line through the origin for our data; (D) best fit regression line.

Table II
Corrected Peak Frequencies and Widths at Half-Peak Height of LAMs for POM Crystals

T_c	ν, cm^{-1} ± 0.3	$\Delta\nu_{1/2}$, cm^{-1} ± 0.4	T_c	ν, cm^{-1} ± 0.3	$\Delta\nu_{1/2}$, cm^{-1} ± 0.4
130	26.1	5.7	139	21.7	5.2
135	22.6	5.8	142	19.4	4.7

average shift being 0.6 cm^{-1}. The band widths at half-peak height ($\Delta\nu_{1/2}$) of the corrected peaks are also shown in Table II. These half-width values are approximately the same size as those reported for polyethylene crystals.[24]

A previous study[25] on the longitudinal acoustic mode of annealed, melt-crystallized POM yields, from a plot of ν vs. L^{-1} (see curve A, Figure 6), $E_c = 203 \pm 6$ GPa. This value was obtained by linear regression through the origin of the data reported in ref 25 (and taking $\rho_c = 1.491$ gm/cm^3) and is slightly different than that reported in that publication. The errors on E_c refer to the standard deviation of the slope of the regression line. This value for E_c agrees quite well with that derived from inelastic neutron-scattering experiments (i.e., 164 GPa[27]) which are considered to provide a correct estimate of the ultimate crystalline modulus.[4]

As discussed in the introduction, the LAM is envisioned as being essentially decoupled at the crystal-fold surface interface and, hence, it is more appropriate to analyze plots of ν vs. $1/l_c$ when attempting to estimate E_c. Recall that for melt-crystallized materials, L reflects the long period which includes contributions from l_c, the fold surface thickness and the thickness of the zone of amorphous material residing between lamellae. l_c is unknown for the materials used in ref 25; for the sake of illustration, we assume that $l_c = L - 50$ Å is a reasonable estimate. Linear regression of the data through the origin (see curve B, Figure 6) yields $E_c = 101 \pm 6$ GPA, about one-half of the value derived from a plot of ν vs. L^{-1}. In addition to the variability introduced through estimation of l_c, one must take great care, especially in the case of melt-crystallized materials, to perform the appropriate SAXS and LAM corrections. For example, Snyder and Scherer[8] have shown that the change in peak frequency as a result of temperature and frequency corrections can be as large as 5 to 10 cm^{-1} depending on the breadth of the LAM. In general, the broader the LAM the larger the change in apparent peak frequency upon correction. This discussion serves to illustrate the sensitivity of the derived E_c to the specific parameters used in the analysis and, if great care is not taken, one would be forced to consider reported values with suspicion.

The plot of our LAM data for single crystals vs. $1/l_c$ is also shown in Figure 6. l_c was estimated from $l_c = L - l_a$ where l_a was chosen as 18 Å and we assume that the chain axis is perpendicular to the fold surface. Linear regression through the origin (line C) yields $E_c = 146 \pm 12$ GPa, in excellent agreement with the results from neutron scattering. However, line C is clearly not the best fit to experimental data. In fact, statistical analysis suggests that a line through the data points, to within 97.5% confidence, should not contain the origin. If we relax the constraint that the regression line must pass through the origin, we obtain $E_c = 55 \pm 10$ GPa and a y intercept of 8.8 cm^{-1}. This nonzero intercept is clearly inconsistent with the simple elastic rod model but considering that we have only four data points, it would be premature to draw any sweeping conclusions. Moreover, if the data point corresponding to the largest $1/l_c$ value was in error, a reasonable straight line through the origin could be constructed.

Finally, to illustrate again the sensitivity of E_c to the values of l_c used in the analysis we examined a plot of ν vs. L^{-1} for our single crystals. Linear regression through the origin yields $E_c = 231 \pm 8$ GPa, a value about 60% higher than that calculated with $l_c = L - 18$ Å. Our results indicate the need for a more extensive investigation into this potentially powerful technique, particularly the need for careful experimental data.

Conclusions

Dual melting points were observed for solution-crystallized POM and the behavior was found to fit well with a mechanism in which the original crystals melt, recrystallize, and then remelt during heating in the DSC. Analysis of the melting points via a Hoffman–Weeks analysis (assuming that T_{m_1} obtained at a heating rate of 20 deg/min is a reasonable approximation for the true T_m) yields $T_m^\circ = 177$–180 °C. In addition, we found $\sigma_e = 88$ ergs/cm^2 and, from this, a work of chain folding near 4 cal/mol folds, a value approximately in line with that for other polyethers. Indirect evidence suggests a value of ΔH_f° near 59 cal/g to be appropriate for poly(oxymethylene).

Assuming that the simple elastic rod model provides an adequate description of polymeric LAM's, we found $E_c = 146 \pm 12$ GPa, in good agreement with the results from neutron-scattering experiments. Model calculations illustrate that the choice of the value used for the length parameter in eq 1, among other factors, is critical and careful measurements/estimates are required before reliable values of the ultimate modulus can be extracted from LAM data.

Acknowledgment. We thank Drs. Ian Harrison and John Rabolt for a number of helpful discussions. We also thank Dr. Randy W. Snyder and Dr. William Varnell for assistance with the LAM and SAXS measurements.

Registry No. Delrin 500, 37273-87-3.

References and Notes

(1) Mizushima, S.; Shimanouchi, T. *J. Am. Chem. Soc.* **1949**, *71*, 1320.
(2) Rabolt, J. F. *CRC Crit. Rev. Solid State Mater. Sci.* **1985**, *12*, 165.
(3) Peterlin, A. *J. Appl. Phys.* **1979**, *50*, 838.
(4) Fanconi, B.; Rabolt, J. F. *J. Polym. Sci., Polym. Phys. Ed.* **1985**, *23*, 1201.
(5) Brew, B.; Clements, J.; Davies, G. R.; Jakeways, R.; Ward, I. M. *J. Polym. Sci., Polym. Phys. Ed.* **1979**, *17*, 351.
(6) Khoury, F.; Barnes, J. D. *J. Res. Natl. Bur. Stand., Sect. A* **1974**, *78A*, 95.
(7) Snyder, R. G.; Krause, S. J.; Schrerer, J. R. *J. Polym. Sci., Polym. Phys. Ed.* **1978**, *16*, 1593.
(8) Snyder, R. G.; Scherer, J. R. *J. Polym. Sci., Polym. Phys. Ed.* **1980**, *18*, 421.
(9) Harrison, I. R.; Runt, J. *J. Polym. Sci., Polym. Phys. Ed.* **1979**, *17*, 321.
(10) Varnell, W. D.; Runt, J.; Harrison, I. R. *J. Polym. Sci., Polym. Phys. Ed.* **1981**, *19*, 1923.

(11) Jaffe, M.; Wunderlich, B. *Kolloid Z. Z. Polym.* **1967**, 216–217, 203.
(12) Rim, P. B.; Runt, J. *Macromolecules* **1983**, *16*, 762.
(13) Harrison, I. R.; Landes, B. *J. Macromol. Sci., Phys.* **1983–1984**, *B22*, 747.
(14) Hoffman, J. D.; Weeks, J. J. *J. Res. Natl. Bur. Stand., Sect. A* **1962**, *66A*, 13.
(15) Wunderlich, B. *Macromolecular Physics*; Academic: New York, 1980; Vol. 3.
(16) Rybnikar, F. *Collect. Czech. Chem. Commun.* **1966**, *31*, 4080.
(17) Amano, T.; Fischer, E. W.; Hinricksen, G. *J. Macromol. Sci., Phys.* **1969**, *B3*, 209.
(18) Inoue, M. *J. Polym. Sci., Part A* **1963**, *1*, 2697.
(19) Korenga, T.; Hamada, F.; Nakajima, A. *Polym. J.* **1972**, *3*, 21.
(20) Wilski, H. *Kolloid Z. Z. Polym.* **1971**, *248*, 867.
(21) Iguchi, M. *Makromol. Chem.* **1976**, *177*, 549.
(22) Hoffman, J. D. *Polymer* **1983**, *24*, 3.
(23) Hoffman, J. D.; Davis, G. T.; Lauritzen, J. I. In *Treatise on Solid State Chemistry*; Hannay, N. B., Ed.; Plenum: New York, 1975; Vol. 3.
(24) Runt, J.; Harrison, I. R. *J. Macromol. Sci., Phys.* **1980**, *B18*, 83.
(25) Rabolt, J. F.; Fanconi, B. *J. Polym. Sci., Polym. Lett. Ed.* **1977**, *15*, 121.
(26) Uchida, L.; Tadokoro, H. *J. Polym. Sci., Polym. Phys. Ed.* **1967**, *5*, 63.
(27) Anderson, M. R.; Harryman, M. B. M.; Steinman, D. K.; White, J. W.; Currat, R. *Polymer* **1982**, *23*, 569.

Surface Ordering Phenomena in Block Copolymer Melts

Glenn H. Fredrickson

AT&T Bell Laboratories, Murray Hill, New Jersey 07974. *Received March 10, 1987*

ABSTRACT: A mean field theory is presented to describe surface ordering phenomena in diblock copolymers near the microphase separation transition (MST). We consider a near-symmetric diblock melt in the vicinity of a solid wall or free surface, such as a film–air interface. The surface is allowed to modify the Flory interaction parameter and the chemical potential in the adjacent copolymer layer. The composition profile normal to the surface is investigated both above and below the MST. In contrast to the surface critical behavior of binary fluids or polymer blends, we find interesting oscillatory profiles in copolymers that arise from the connectivity of the blocks. These composition profiles might be amenable to study by ellipsometry, by evanescent wave-induced fluorescence, or by scattering techniques. Wetting and other surface phenomena and transitions in block copolymers are briefly discussed.

1. Introduction

Block copolymers constitute one of the most interesting classes of synthetic high-polymer materials and have great potential for specialty and high-technology applications. An important factor that contributes to the utility of block copolymers is that their macroscopic properties can be carefully tailored during synthesis by controlling molecular weight and composition. For a good introduction to the static and dynamic properties of block copolymers as well as their applications, we refer the interested reader to ref 1 and 2.

The vast majority of both experimental[1–8] and theoretical[9–18] investigations of molten block copolymers have dealt with the bulk properties of these materials. Much of this work has focused on the microphase separation transition (MST), at which a block copolymer forms spatially periodic ordered microphases. Starting with a disordered block copolymer, the MST can be approached either by lowering temperature or by stripping off a low molecular weight solvent that has been added to the copolymer melt to enhance miscibility and lower viscosity. The type of ordered morphology that forms at the MST depends on the composition and molecular architecture of the copolymer, but frequently encountered morphologies include one-dimensional lamellae, hexagonal packings of cylinders, and body-centered-cubic (BCC) arrays of spheres.

The theories for the equilibrium properties of block copolymers can be divided into two classes. The first class, the weak segregation limit theories,[10,14,17] are believed to be applicable to the disordered phase of copolymers and to the ordered microphases at temperatures very near the MST. They assume low amplitude composition patterns with no sharp interfaces between microdomains. Such theories make predictions for the location of the MST (in the parameter space of temperature, molecular weight, and composition) and for radiation scattering in the disordered phase. These predictions are in reasonable qualitative agreement with experiment, although some quantitative discrepancies have been found.[3,7] The second class of theories is the strong segregation limit theories,[9,11–13] which are applicable to well-developed ordered microdomains. These theories are believed to be most accurate at low temperature when the widths of the interfaces between microdomains are narrow relative to the size of a domain. The strong segregation theories are also in reasonable agreement with experiment.[3,6,7]

Recently, kinetic theories have been developed to describe the low-frequency dynamics of block copolymers in the vicinity of the MST.[15,16,18,36] These theories are dynamical extensions of the weak segregation limit equilibrium theories discussed above. They make predictions for the radiation scattering from diblocks under steady flow fields,[15] for the linear viscoelastic properties of disordered melts near the MST,[16,36] and for the early stages of the ordering dynamics following a quench across the MST.[18] Unfortunately, there has been much less experimental work on the dynamics of block copolymers, so few of these predictions have been tested in the laboratory.

All of the above-mentioned theories and experiments have focused on the *bulk* static or dynamic properties of block copolymers, i.e., the macroscopic and fluctuation properties far from any bounding surfaces or interfaces. In contrast, there have been only a handful of experimental studies on the behavior of block copolymers near surfaces.[19–21] Furthermore, we are not aware of any theoretical work on the equilibrium or kinetic surface properties of molten block copolymers. Because block copolymers are finding increasing applications as thin films, adhesives, and surfactants, it would seem that a fundamental understanding of their surface phenomena is essential.

The present paper is a contribution to the equilibrium theory of block copolymers near a surface. For simplicity we consider a diblock copolymer melt that orders into the lamellar morphology at the MST. Hence, we restrict consideration to symmetric or nearly symmetric A–B di-

0024-9297/87/2220-2535$01.50/0